PNC-TN941 82-189

Temperature Rise due to Fission Gas Release in Locally Blocked LMFBR Fuel Subassembly Simulators

August, 1982

OARAI ENGINEERING CENTER

POWER REACTOR AND NUCLEAR FUEL DEVELOPMENT CORPORATION

and

TOSHIBA CORPORATION

PNC-TN941 82-189
1982 年 8 月

局所閉塞されたLMFBR模擬燃料集合体での FPガス放出による温度上昇

羽賀 一男*，山口 勝久*
名女川 文比古**

要 旨

LMFBR燃料集合体において，局所流路閉塞と燃料ピンからのFPガス放出が重ね合わされた場合の閉塞物後流での温度上昇について，実験的検討を行なった。

用いられた37本組試験体は「グリッドスペーサ型中心閉塞」，「グリッドスペーサ型片側閉塞」，「ワイヤスペーサ型中心閉塞」の3体である。これらの試験結果の相互比較により，閉塞物後流での冷却能力に影響を与えるガス放出率，ナトリウム流速，スペーサ形式，閉塞物位置等の効果を調べた。測定された温度上昇はワイヤスペーサ型中心閉塞の場合とグリッドスペーサ型片側閉塞の場合でほぼ等しく，ガス放出による温度上昇には体系，流動条件に依らず上限値があることがわかった。本試験結果をもとに実機条件でのガス放出による温度上昇を評価した。

なお，本報告書は1982年リオン市で開かれた「液体金属高速増殖炉の安全性，設計および運転に関する国際会議」における発表の予稿と同一のものである。

* 大洗工学センター，高速炉安全工学部，炉心安全工学室
** 東京芝浦電気(株)，原子力技術研究所

PNC-TN941 82-189
Aug. 1982

Paper submitted to the International Topical Meeting on Liquid Metal Fast Breeder Reactor Safety and Related Design and Operational Aspects, Lyon, July 19/23, 1982.

TEMPERATURE RISE DUE TO FISSION GAS RELEASE IN LOCALLY BLOCKED LMFBR FUEL SUBASSEMBLY SIMULATORS

K. Haga, K. Yamaguchi

O-arai Engineering Center, Power Reactor and Nuclear Fuel Development Corporation
O-arai, Ibaraki-ken, 311-13, Japan

F. Namekawa

Nuclear Engineering Laboratory, Toshiba Corporation
Kawasaki-ku, kawasaki, 210, Japan

ABSTRACT

The combined thermal effects of local blockage and fission product gas release in an LMFBR fuel subassembly were investigated in the present study. The temperature rise in the wake region was measured in out-of-pile experiments using three sets of electrically heated 37-pin bundles cooled by sodium. From the test results the influence of the main factors which govern the cooling capability of the blocked bundle, such as gas release rate, sodium flow rate, spacer type and blockage location, was examined. The temperature rise due to gas release in the central blocked wire-spacer bundle was almost identical to that in the edge blocked grid-spacer bundle. From these results the wake temperature rise in the case of gas release under reactor operating conditions was estimated.

INTRODUCTION

It is generally believed that a local blockage in a fuel subassembly of a Liquid Metal Fast Breeder Reactor (LMFBR) would be a possible initiator of pin-to-pin failure propagation because of the close arrangement of the pins. Considerable research and development (R&D) programs on the local cooling disturbance, such as the study by Yamaguchi et al [1], have indicated that local boiling would take place under the situation of a large blockage with a certain power-to-flow mismatch. Even if the local boiling condition is not reached, the increase in cladding temperature is large enough to lead to a reduction in cladding mechanical strength. The internal pressurization by fission product (FP) gases, which increase with fuel burn up, will raise the possibility of cladding rupture. The FP gas release resulting from the pin rupture would disturb the cooling performance of the surrounding pins and might lead to pin-to-pin failure propagation. Therefore, it is of great importance in the safety assurance of an LMFBR, to evaluate the potential for this failure propagation within the locally blocked fuel subassembly.

The sodium experiments on the FP gas release in a normal bundle have been reported by Wilson et al [2] and Haga et al [3]. But their results would not apply in the evaluation study of FP gas release into the locally blocked fuel subassembly, because the flow condition in the wake region is quite different. Table I shows the main factors which would govern the temperature rise in the case of FP gas release behind a blockage.

Namekawa et al [4] conducted FP gas release experiments in a wire-wrapped 37-pin bundle whose central 24 subchannels were blocked. In addition, the authors [5] performed similar gas release experiments using two grid-spacer pin bundles one blocked by a central blockage and another by an edge blockage. Based on these experimental data, we have examined the effect of each factor shown in Table I. However, because impermeable blockages were adopted in the same pin arrangement bundles and a single gas species was used, items A-1, B-1 and C-2 in the table were not covered in these experiments.

EXPERIMENTAL METHOD

Test Section

Three series of out-of-pile experiments were carried out with the Sodium Boiling and Fuel Failure Propagation Test Facility, SIENA [1], at the O-arai Engineering Center of the Power Reactor and Nuclear Fuel Development Corporation (OEC/PNC).

The experiments were conducted in three of 37-pin bundles installed in turn in the facility. Table II shows the summary of the pin bundle geometries.

In the test sections named "37GC" and "37WC", the central 24 subchannels were blocked by a stainless steel plate near the middle position of the heated sections, and in the one called "37GE" a half edge part (39 subchannels) of the total flow area was blocked by the same material. In these bundles, eighteen pins in the blocked region were electrically heated sheath-type heater pins. The heated zone length was about 460 mm and the heat flux was uniform. Each bundle was contained within a hexagonal wrapper tube whose flat-to-flat distance was 50.4 mm.

The pins (6.5 mm in diameter) were spaced with a 7.9 mm pitch by 1.3 mm diameter wrapping wires in 37WC and by honeycomb type grid spacers in 37GC and 37GE, in which blockages were located at the leading end planes of the 15 mm high grid spacers.

Argon was used as a simulant FP gas. It was in most cases released from a gas injector pin, which was inserted into the test section as a center pin of the bundle.

The pin bundle cross sections of the 37GE are shown in Fig. 1. In some runs using this test section, gas was released from a nozzle of the duct wall instead of the central gas injector pin. Three gas injector pins were prepared to inject gas, each through a nozzle of different diameter (0.3 mm, 0.5 mm and 0.8 mm).

Pin surface temperatures were measured with 0.3 mm diameter thermocouples embedded in the heater cladding. On the other hand sodium temperatures were measured with the same diameter thermocouples immersed in the subchnnel centers. Void fractions within the pin bundles were measured with resistivetype void-meters, which deduced volume averaged void fractions between planes where the potential taps were mounted along the wrapper tube wall. The sodium flow rates entering into and coming out of the test bundle were measured with electromagnetic flow-meters attached at the subassembly inlet and outlet. A pressure transducer was installed at the gas plenum.

Test Procedure

The first test was a single shot of transient gas release carried out by breaking a fresh rupture film in the gas injector pin. A constant volume of gas in the gas plenum, whose volume was 70 cm^3 or about twice of that of a MONJU fuel pin, was released during the test. Then, a series of steady gas release runs followed, where a regulator valve at the outlet of a gas cylinder was used to adjust the gas release rate. The gas temperature was initially adjusted to be the same as the test section inlet sodium temperature.

Table III gives the test parameter ranges of all runs. The heat flux was held relatively low to avoid sodium boiling or possible pin deformation due to gas blanketing. The proportional correlation between heat flux and temperature rise under gas release conditions has been shown in the previous experiments [4].

EXPERIMENTAL RESULTS AND DISCUSSIONS

Steady Gas Release Runs

Typical axial temperature profiles behind the 37GC and 37GE blockage under steady gas release conditions are shown in Figs. 2 and 3, respectively.

Except for the difference in the nozzle diameter, 0.5 mm in Fig. 2 and 0.3 mm in Fig. 3, experimental conditions were almost identical in both runs. The figures show that the gas release caused additional temperature rise relative to that without gas release. Especially in 37GE the temperature rise is marked and the high temperature zone extends more than 80 mm from the blockage. These findings mean that the released gas is easily trapped in the axial long wake region of an edge blockage.

Effects of Gas Plenum Pressure and Gas Injection Nozzle Diameter

Figure 4 shows the correlation between gas plenum pressure and temperature rise behind a blockage in 37GE. At the gas injection plane of Z = 22 mm, the temperature rise took the maximum value when the gas plenum pressure was 1.2 MPa, then it showed a decreasing tendency with increasing plenum pressure. However, in the downstream planes, the gas plenum pressure at which the temperature rise attained the peak value shifted higher in keeping with the distance from the blockage. There was no significant difference between the maximum temperatures measured in each axial location. This indicates, that there is a limit in the gas concentration behind the blockage. Furthermore, from the above data it should be expected that the temperature rise is governed by the gas release rate rather than by the gas plenum pressure. The same effect can be found on the gas release nozzle diameter [4], that is, the only nozzle diameter effect is that it controls the gas release rate.

Effects of Sodium Velocity and Gas Release Rate

The familiar normalized temperature rise was introduced to intercompare the local cooling disturbances under various thermohydraulic conditions:

$$\Theta = \frac{d_h}{4} \cdot c_p \rho \cdot (T - T_{core}) \cdot \frac{U_B}{q''} \quad . \qquad (1)$$

Under the convection controlled heat transfer assumption, the physical meaning of the normalized temperature rise is the integrated axial distance of flowing sodium which is required for the sodium to attain the same temperature rise as the intra-wake rise in the normal bundle (without blockage) with other conditions being equal. The enthalpy rise in the sodium within the wake is, therefore, proportional to the value of the normalized temperature rise.

Figure 5 shows an example of the normalized temperature rise data calculated from Eq. (1) and pin surface temperature readings at Z = 52 mm in 37GE. The sodium velocity at the blocked plane is taken as the horizontal axis and the gas release rate, as a parameter. The observed tendency in this figure, that the temperature rise becomes higher with the gas release rate, is the same as those seen in 37GC and 37WC.

The normalized temperature rise data shown in Fig. 5 are rearranged in Fig. 6 to examine the effect of the gas release rate G_g. Here, the core flow velocity at the blocked plane is taken as a parameter. The normalized temperature rise data at high flow rate conditions show abrupt increases in the narrow ranges of gas release rates up to 0.6 g/s (1 g/s = 556.8 Ncm^3/s). Beyond this point, they slightly decrease with increasing gas release rate. Two reasons are given to explain the reduction of temperature rise data at $G_g > 0.6$ g/s range: (a) there is an upper limit to the total amount of gas that can accumulate within the wake region, which will be given by the geometrical limit of the wake volume and the phenomenological limit of the slip ratio between sodium velocity and bubble velocity, (b) the increase of the gas release rate produces an intensified gas jet and an associated sodium flow both of which have sufficient inertia to break the wake partially and wash the accumulated gas out of the wake region with the accompanying replacement by sodium.

Transient Gas Release Runs

The general effects of gas release behind a blockage were revealed from the above steady release runs. However in the possible gas release in a fuel subassembly, FP gas would be released transiently from failed fuel pins. The transient phenomena may add an unexpected effect on the thermohydraulics behind a blockage under gas release condition. To examine this effect, several transient gas release runs were conducted in each experiment.

Figure 7 shows typical signals of gas release rate, temperature, void fractions and sodium velocities measured during Run GLE-3 of the 37GE experiment. In this case gas was released from the center pin to the wake region behind an edge blockage. At the start of gas release the inlet flow velocity reduced temporarily. The signal of void-meter VoT-4 located just behind the blockage was smaller than that during the latter half of the transient.

This indicates that the gas bubble is not so effectively trapped when the gas release rate is large. As observed in the steady tests, the pin surface temperature was higher at Z = 52 mm than at Z = 22 mm. The temperature rise 22 mm downstream from the blockage increased with the decrease in the gas release rate. This tendency coincided well with the increase in the void fraction just behind the blockage. About 5.2 seconds after the start of the transient the valve between the gas plenum and the gas supply line was opened. Temperatures dropped to the same levels observed under the steady gas release run with the same gas release rate because the high pressure gas was continuously provided.

The following is concluded to summarize the results of transient runs: (a) The maximum temperature rise during transient gas release was approximately the same as that during steady release runs, (b) the temperature rise is influenced solely by the gas volume and gas concentration accumulated in the wake and is independent of the momentary gas release rate.

The fact that there was no fundamental difference between the peak temperatures under transient gas release and those under steady gas release, shows that the plentiful steady release run data can be used for the evaluation of the thermal effect of FP gas release in a fuel subassembly.

Effect of Bundle Geometry

Figure 8 is a summary of the effects of gas release rates on the normalized temperature increases during steady gas release runs in four test conditions. Gas injector pins were used to supply argon behind the central blockage of the wire wrapped bundle (Case 1) and the grid spacer bundle (Case 2). In the edge blockage test section with a grid spacer, gas was released from the center pin (Case 3) or from the duct wall (Case 4). Except for Case 2, the temperature rise curves are quite similar to each other. This proves that there is an upper limit to the gas contained in the wake region. The low temperature rise in Case 2 was caused by the ease of gas escape out of the wake region due to the short distance from the gas injection nozzle to the edge of the blockage and the lack of obstacles such as spacer wires.

Effects of Other Factors

In this section the remaining factors listed in Table I are examined briefly.

The <u>pin pitch / pin diameter ratio</u> of fuel subassemblies are compared in Table IV for some LMFBRs. It is seen that the MONJU fuel subassembly, whose dimensions are the same as those in the present test sections, has the second smallest p/d values in the table. The experimental data described above, therefore, might correspond to the sever case that would occur in the actual fuel subassemblies because the released gas behind a blockage would be easily trapped due to the relative tightness of the pin arrangement.

The effects of <u>permeable</u> blockage on the gas accumulation was investigated by Fukuzawa [6] in water experiments. He found that the size and the residence time of the gas cavity decreased with increasing leakage flow and that above a leakage ratio of about 5%, a gas cavity was not seriously observed behind the 21%-corner blockage.

The gas release experiments by Wilson et al [2] were conducted changing the gas temperature widely with different gas species. Some runs in their normal three pin bundle were performed, in which 720°C gases were injected, while 510°C gases were used in the other runs. As to the gas species, although they used argon as FP gas simulant in most cases, xenon was released in selected runs. However they found little difference in the pin surface temperatures between the two cases.

Extrapolation to Reactor Conditions

In order to evaluate the coolability of a reactor fuel subassembly under FP gas release behind a blockage, the normalized temperature rise data shown in Fig. 8 can be extrapolated with the following equation:

$$T - T_{core} = \Theta_{ref} \cdot \left(\frac{4q''}{d_h \cdot c_p \rho \cdot U_B} \right) \qquad (2)$$

From Eq. (2) and directly from the curve of Case 1 in Fig. 8, the temperature rise behind a 24-subchannel blockage under gas release conditions in a MONJU fuel subassembly (i.e., 6% central-type blockage of 169-pin bundle) was estimated in [4]. The calculated results indicated that the temperature rise due to gas release would exceed 1000°C for a wide range of gas release rates.

To make the quantitative evaluation more accurate, however, the difference in density between actual FP gas and argon and the difference in system pressure between reactor core and test sections should be taken into account. The density of xenon, which is the main component of FP gas, is about three times that of argon. Furthermore the absolute system pressure of the reactor core region is higher than that of the heated section in the present pin bundles (approximately 0.2 MPa) by three or four times. Considering these differences in estimating the temperature increases in fuel subassemblies from Fig. 8, the values of the horizontal axis must be multiplied by one order of magnitude to have the same volumetric flow rate as in these tests. Another point is whether or not the FP gas in the gas plenum can easily pass through the gap between fuel and cladding.

Although, as mentioned above, the situation in the practical reactor core differs a little from the present experiments, the possibility of a temperature rise which is high enough to cause temporary sodium boiling in a fuel subassembly cannot be excluded.

There is little useful information on the sodium boiling heat removal capability under the presence of entrained FP gas, while Bishop et al [7] have examined the similar problem under the two-component two-phase condition. The improvement of the boiling heat transfer performance in the presence of noncondensable gas is unlikely. A proposed dryout criterion without gas release, namely attaining the high enthalpy condition which satisfies the theoretical excess temperature of more than a few hundred degree C over the saturation temperature, will therefore give the conditions sufficient for pin failure. The FP gas release associated with the small blockage has, therefore, the potential for causing inside-wake pin-to-pin failure propagation. However, as was noted earlier, the significant temperature rise which causes dryout is restricted to within the gas accumulation region.

The temperature outside this gas accumulation region would be of the same magnitude as the one observed in the normal bundle gas release results [3]. Hence, the pin-to-pin failure propagation would be limited to a part of the blockage wake region, even if local dryout is caused by gas accumulation. It is expected that in-core monitors, such as eddy current flow-meters, can detect pin failure [8].

CONCLUSIONS

Based on the gas release experiments behind blockage in three sets of 37-pin bundles, the following conclusions were obtained.

(1) In general the temperature rise was higher (i) in the wire spacer bundle than in the grid spacer bundle, and (ii) behind the edge blockage than behind the central blockage.

(2) Except for the centrally blocked grid-spacer bundle, the upper limit of the temperature rise and the gas release rate at which the maximum temperature value was obtained were almost identical, independent of the type of spacer, blockage and gas injection point.

(3) There was a tendency that the higher the sodium flow was the higher was the temperature rise.

(4) The empirical correlation to estimate the temperature rise was found from the test results. It was deduced that FP gas release in the LMFBR fuel subassemblies with a local blockage has a potential to cause a limited pin-to-pin failure propagation in the wake region.

To confirm these conclusions, a series of gas release experiments in a 91-pin bundle is being prepared by PNC.

NOMENCLATURE

c_p = specific heat capacity for sodium
D = gas release nozzle diameter
d_h = subchannel hydraulic equivalent diameter
G_g = gas release rate
P_g = gas plenum pressure
P_{go} = initial gas plenum pressure
q'' = heat flux
T = temperature
t = time since gas injection
T_{core} = temperature at core flow region
T_{in} = inlet sodium temperature
U_B = sodium velocity at blocked section
U_{in} = inlet sodium velocity
Z = distance from blockage
ρ = density
Θ = normalized temperature rise, Eq. (1)
Θ_{ref} = normalized temperature rise in reference case

ACKNOWLEDGMENTS

The authors are indebted to Messrs. T. Isozaki, T. Komaba, M. Uotani, K. Sahashi, Y. Daigo, Y. Kikuchi and A. Ohtsubo for their engineering and technical contributions throughout the performance of individual experiments. The authors particularly wish to express their thanks to Dr. C. L. Larson for his useful advice and effort on manuscript preparation.

REFERENCES

1. K. Yamaguchi et al., "Experimental Investigation of Local Cooling Disturbances in LMFBR Fuel Subassemblies," ASME Winter Annual Meeting, 81-WA/HT-40 (1981).
2. R.E. Wilson et al., "Experimental Evaluation of Fission Gas Release in LMFBR Subassemblies Using Electrically Heated Test Section with Sodium as Coolant," ANL-8036 (1973).
3. K. Haga et al., "Fission Gas Release Experiment in a Simulated LMFBR Subassembly," Trans. Am. Nucl. Soc., 34, 494 (1980).
4. F. Namekawa, K. Yamaguchi and K. Haga, "Out-of-Pile Experiments for Fission Gas Release in LMFBR Fuel Subassemblies—Gas Release into Blockage Wake Region with a Wire-Wrapped 37-pin Bundle," ASME Winter Annual Meeting, 81-WA/HT-62 (1981).
5. K. Haga, K. Yamaguchi and F. Namekawa, "Experimental Study on the Effect of Fission Product Gas Release into Blockage Wake Region Using a Simulated LMFBR Fuel Subassembly," Nucl. Eng. Design (submitted for publication).
6. Y. Fukuzawa, "Influence of Leakage Flow on the Behaviour of Gas Behind a Blockage in LMFBR Subassembly Geometry," KfK-2969 (1980).
7. A. Bishop, A. Engel and R.A. Markley, "Heat Transfer Effect on Entrained Gas in Liquid Sodium Systems," Nucl. Eng. Design, 52, 1 (1979).
8. T. Ogino et al. "Feasibility Study of Local Core Anomaly Detection by Use of Temperature and Flow Fluctuations at LMFBR Fuel Subassembly Outlet," in Proc. International Meeting on Fast Reactor Safety Technology, Seattle (1979), p. 2630.

TABLE I

Main Factors which Govern the Temperature Rise Behind Blockage in the Case of Fission Gas Release

A. Geometry	A-1. Pin pitch/Pin diameter A-2. Spacer type (Grid or Wire)
B. Blockage Situation	B-1. Permeable or Impermeable B-2. Location (Central subchannels or Edge subchannels)
C. Gas Release Situation	C-1. Gas release rate C-2. Gas species and gas temperature
D. Operating Conditions	D-1. Sodium flow rate D-2. Heat flux

TABLE II

Summary of the Pin Bundle Geometries

Pin bundle		37GC	37GE	37WC	MONJU
Pins		37	37	37	169
(Heaters)		(18)	(18)	(18)	--
Tie rods*		18	18	—	--
Heated section length	(mm)	456	460	455	930
Blocked location**	(mm)	304	308	300	--
Blockage thickness	(mm)	5	5	5	--
Wrapper tube width	(mm)	50.4	50.4	50.4	104.6
Wrapper tube thickness	(mm)	10	10	10	3
Pin diameter	(mm)	6.5	6.5	6.5	6.5
Pin pitch	(mm)	7.9	7.9	7.9	7.87
Flow area	(mm^2)	915.5	915.5	924.3	3636.1
Hydraulic diameter	(mm)	3.51	3.51	3.43	3.22
Blockage type		central	edge	central	--
Blocked subchannels	(-)	24	39	24	--
Blockage ratio***	(-)	0.39	0.58	0.26	--
Height of grid spacer	(mm)	15	15	--	--
Spacer wire diameter	(mm)	--	--	1.3	1.32
Axial pitch of spacer	(mm)	200	200	265	307

* Diameter of each tie rod is 2.0 mm.
** Distance from the bottom of heated section to the downstream end of blockage.
*** Cross section of grid is considered as blockage.

TABLE III

Experimental conditions

Item	Steady gas release	Transient gas release
Gas plenum pressure P_g, MPa	0.3 - 5.9	3.3 - 8.2
Gas release rate G_g, g/s (N cm^3/s)	0.05 - 5.78 (45 - 3240)	—
Gas temperature in gas plenum T_g, °C	245 - 352	245 - 316
Inlet sodium velocity U_{in}, m/s	0.4 - 4.6	3.5 - 3.8
Inlet sodium temperature T_{in}, °C	232 - 308	247 - 291
Heat flux q", W/cm^2	4.0 - 44.2	29.3 - 30.8

TABLE IV

Tightness of Fuel Pin Arrangement in LMFBRs

Reactor	MONJU	SNR-300	CRBRP	PFR	PHÉNIX
Pin diameter d (mm)	6.5	6.0	5.8	5.8	6.6
Pin pitch p (mm)	7.87	7.9	7.3	7.4	7.7
p/d (-)	1.21	1.32	1.22	1.26	1.18

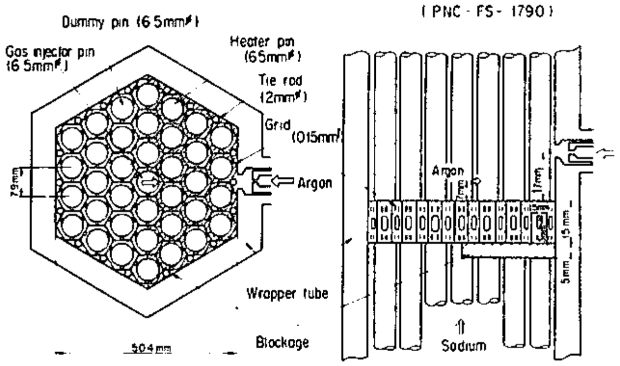

Fig.1 Cross sections of 37GE pin bundle

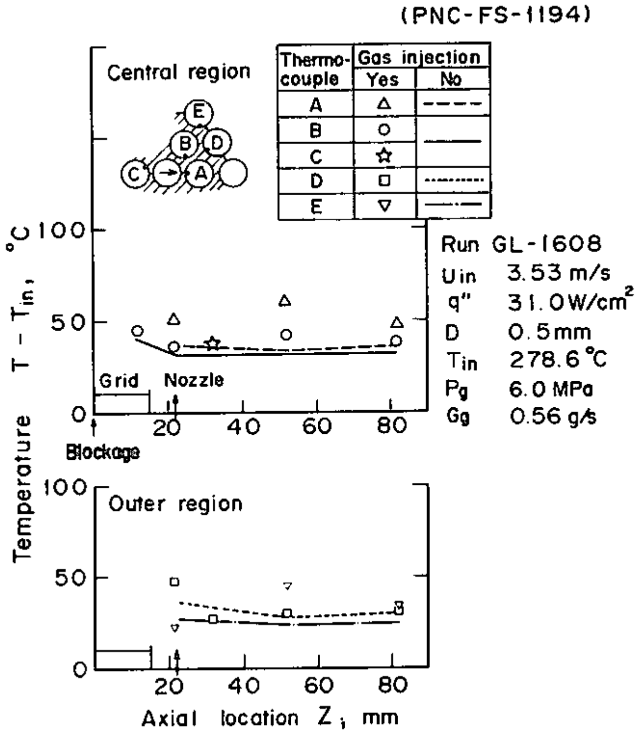

Fig.2 Axial temperature profile; 37GC test section

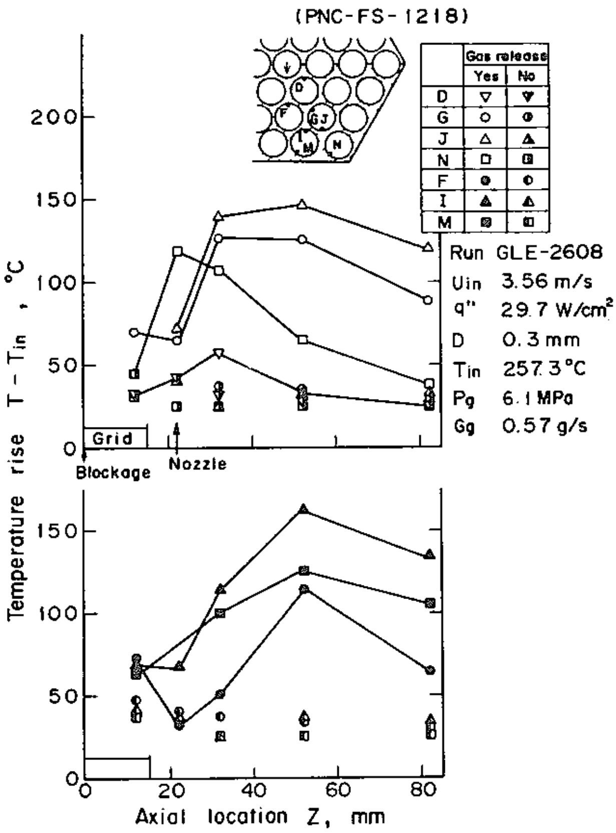

Fig.3 Axial temperature profile; 37GE test section

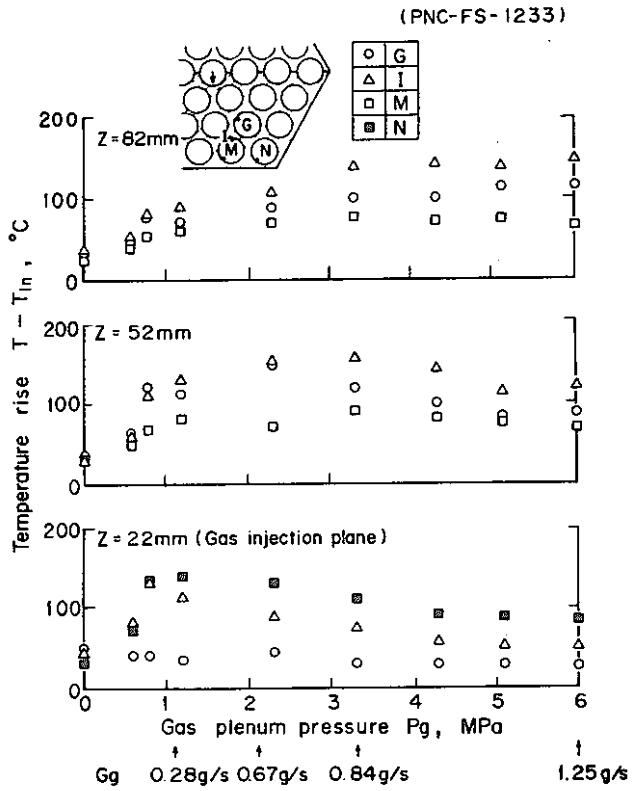

Fig.4 Temperature rise versus gas plenum pressure

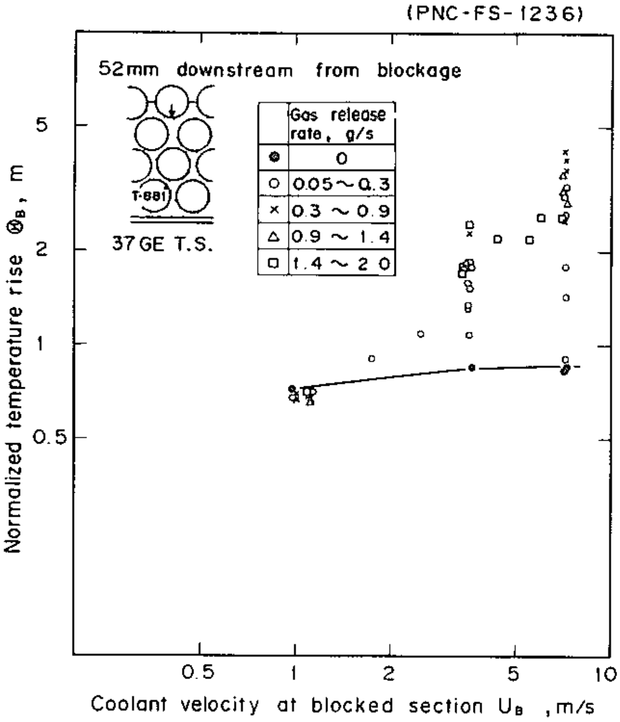

Fig.5 Effect of sodium flow rate on temperature rise behind blockage

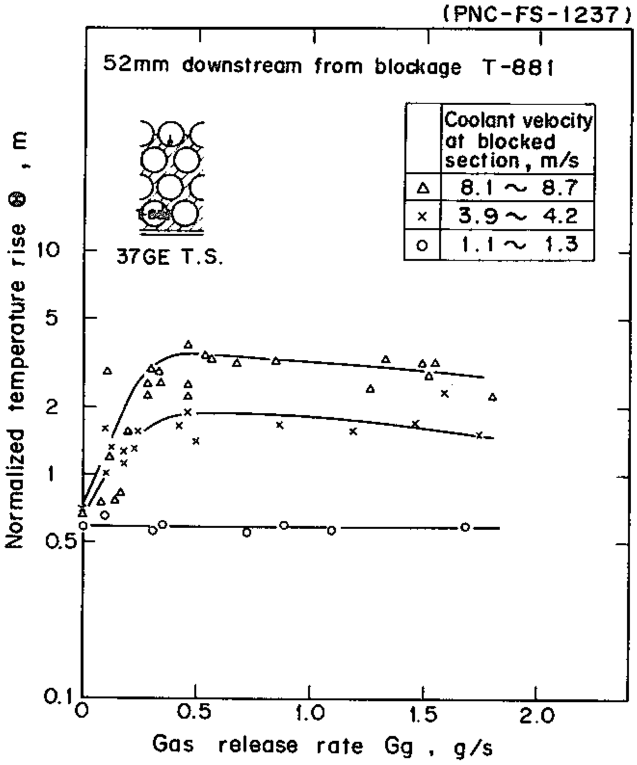

Fig.6 Effect of gas release rate on temperature rise behind blockage

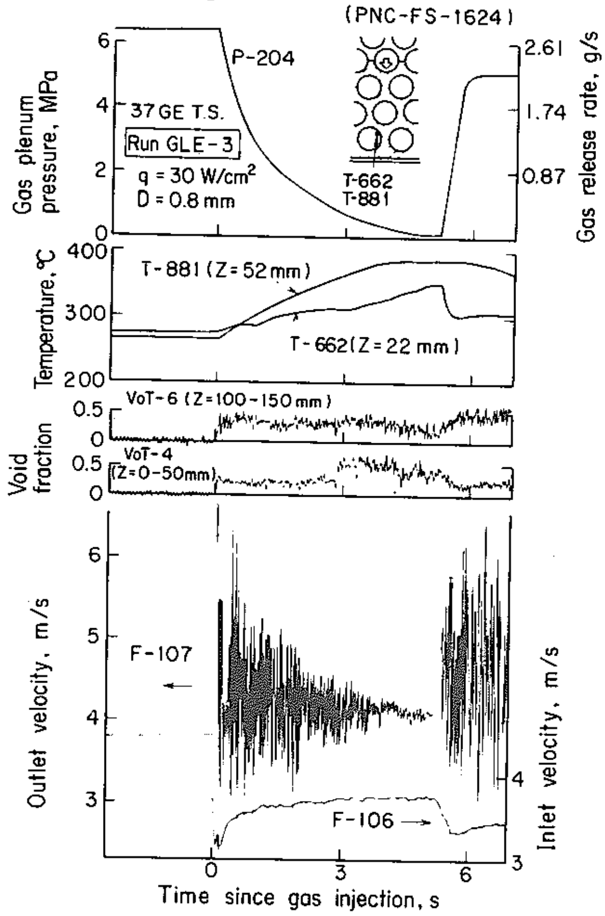

Fig.7 Behavior of gas plenum pressure temperature, void fraction and coolant velocity measured in transient gas release run

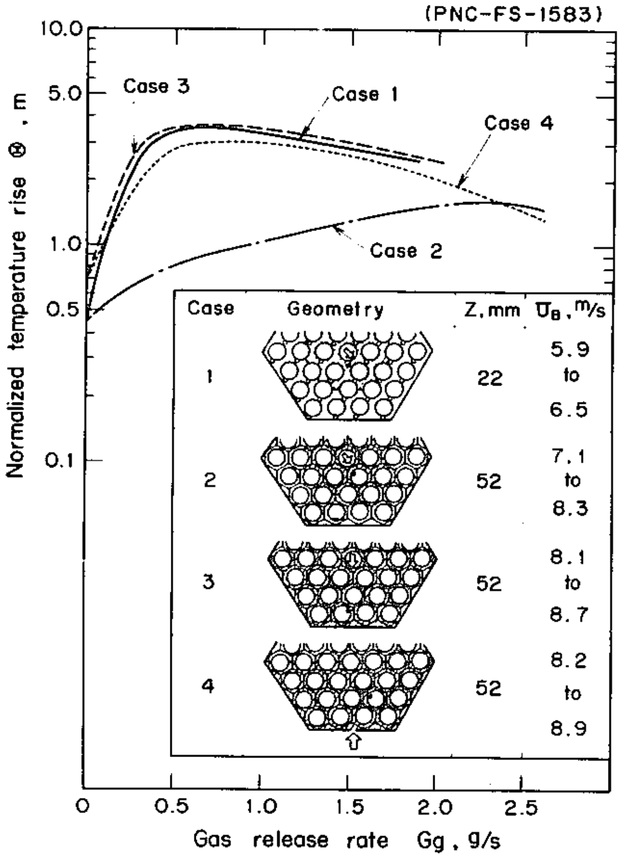

Fig.8 Effect of gas release rate on temperature rise in wake region under various geometrical conditions